R. & M. No. 3093
(19,354)
A.R.C. Technical Report

MINISTRY OF SUPPLY

AERONAUTICAL RESEARCH COUNCIL
REPORTS AND MEMORANDA

Observations of the Flow Patterns of a Two-Dimensional 4 per cent Thick Biconvex Aerofoil at $M_0 = 1 \cdot 40$ and $1 \cdot 63$

By

B. D. HENSHALL, B.Sc., Ph.D., and R. F. CASH, A.F.R.Ae.S.
of the Aerodynamics Division, N.P.L.

LONDON: HER MAJESTY'S STATIONERY OFFICE
1958
PRICE 3*s.* 6*d.* NET

Observations of the Flow Patterns of Two-Dimensional 4 per cent Thick Biconvex Aerofoil at $M_0 = 1 \cdot 40$ and $1 \cdot 63$

By

B. D. Henshall, B.Sc., Ph.D., and R. F. Cash, A.F.R.Ae.S.
of the Aerodynamics Division, N.P.L.

Reports and Memoranda No. 3093*
June, 1957

Summary.—Direct-shadow and schlieren photographs and pressure distributions of the flow past a two-dimensional 4 per cent thick biconvex aerofoil for a limited range of incidences at Mach numbers of $1 \cdot 40$ and $1 \cdot 63$ are presented.

Shock-induced boundary-layer separation at the trailing edge of the aerofoil was present at $M_0 = 1 \cdot 63$ with transition-free boundary layers but was absent up to 5 deg incidence at $M_0 = 1 \cdot 63$ with transition-fixed boundary layers and up to 6 deg incidence at $M_0 = 1 \cdot 40$ with transition-free boundary layers.

1. *Introduction.*—In previous reports[1, 2] investigations of the flow past a two-dimensional 4 per cent thick biconvex aerofoil at subsonic speeds have been made. Recently tests on the same aerofoil at two supersonic speeds, namely free-stream Mach numbers of $1 \cdot 40$ and $1 \cdot 63$, have been completed and the results are presented. In a subsequent paper a description will be given of the testing of this biconvex aerofoil in slotted-wall transonic liners and thus results will be available from low subsonic ($M_0 = 0 \cdot 40$) to moderate supersonic speeds for wide ranges of incidence.

The Reynolds numbers of the current tests, based on the aerofoil chord of 9 in., were approximately $3 \cdot 4 \times 10^6$ and $3 \cdot 5 \times 10^6$ at $M_0 = 1 \cdot 63$ and $1 \cdot 40$ respectively. Throughout this investigation, particular attention was given to the presence (or otherwise) of shock-induced boundary-layer separation at the trailing edge of the aerofoil[3].

2. *Experimental Data.*—2.1. *Results at $M_0 = 1 \cdot 63$.*—Previous experiments on this 4 per cent biconvex aerofoil in the 36-in. × 14-in. High-Speed Wind Tunnel at subsonic speeds[1, 2] had shown that only minute differences existed between tests made with natural (or transition-free) boundary layers and those with transition-fixed boundary layers produced artificially by 5 per cent chord bands of carborundum at the leading edge of the aerofoil. Hence the first series of tests at $M_0 = 1 \cdot 63$ were made using transition-free boundary layers. When shock-induced boundary-layer separation at the trailing edge of the aerofoil was found to be present, a further series of tests were made with transition-fixed boundary layers and in these results no regions of separated flow were observed. Figs. 1 and 2 present the variation of normal-force coefficient C_N and pitching-moment coefficient C_m with incidence at $M_0 = 1 \cdot 63$. Whilst distinct differences exist between the transition-free and the transition-fixed results, the pressure distributions given in Figs. 3 and 4 show that these differences are confined to the trailing-edge region. Schlieren photographs such as Fig. 5 confirm these remarks but the two distinct flow patterns are most clearly illustrated by the direct-shadow photographs presented in Fig. 6. With transition-fixed

---

* Published with permission of the Director, National Physical Laboratory.

boundary layers there is no separation at the trailing edge but with transition-free boundary layers separation is present at $\alpha = 3$ deg and increases in chordwise extent as the incidence is increased. At $\alpha = 5$ deg the separated region extends from 0·95 chord to the trailing edge.

It is of interest to determine the flow deflection which will just cause flow separation. For a circular-arc biconvex aerofoil the trailing-edge semi-angle β is approximately given by

$$\tan \beta \simeq 2 \times \frac{\text{aerofoil thickness}}{\text{aerofoil chord}} .$$

Hence for this 4 per cent biconvex aerofoil

$$\beta \simeq \tan^{-1} \frac{8}{100} \simeq 4°36'.$$

Thus the flow deflection angle θ and the incidence of the aerofoil α are connected by the relation

$$\theta \simeq \alpha + 4°36' \simeq \alpha + 4\tfrac{1}{2}°.$$

Ref. 3 reports an investigation of the interaction between shock waves and boundary layers at the trailing edge of a double-wedge aerofoil at $M_0 = 1·60$. For the transition-free case, where the boundary layer was laminar at separation but turbulent at reattachment to wake, laminar separation was present when $\theta = 5$ deg. For the transition-fixed or turbulent case, turbulent separation was present when $\theta = 12\frac{1}{2}$ deg. Hence, in the present investigation, shock-induced boundary-layer separation might be expected to be observed at $\alpha = 1$ deg in the transition-free case and $\alpha = 8$ deg in the transition-fixed case. However, at $M_0 = 1·63$ the tunnel became choked above $\alpha = 5$ deg and investigation of the turbulent case was impossible. The transition-free results show separated regions present from $\alpha = 3$ deg onwards, that is, $\theta = 7\frac{1}{2}$ deg onwards.

The direct determination of the occurrence of separation by divergence of the trailing-edge pressure[5] was attempted in Fig. 7, but more consistent results were obtained in Fig. 8 where the divergence of the pressure at 0·97 chord was considered (this may be attributed to the diffuse nature of the trailing-edge shock wave in the supersonic case). From these figures it may be deduced that laminar separation is present at $\theta = 7$ deg. The upstream influence of the shock-wave boundary-layer interaction was calculated using the methods of Refs. 3 and 4. When $\alpha = 5$ deg, the extent of this influence is given by $d/\delta_0{}^* = 32$, where

d = distance from trailing edge of beginning of separated region

$\delta_0{}^*$ = calculated boundary-layer displacement thickness at beginning of separated region.

This result is not inconsistent with the findings of Refs. 3 and 4. However, it should be noted that the Reynolds numbers of the present tests are an order of magnitude greater than for the previous tests[3,4].

2.2. *Results at $M_0 = 1·40$*.—The variation of pitching-moment coefficient and normal-force coefficient with incidence at $M_0 = 1·40$ is given in Figs. 1 and 2, and specimen pressure distributions are presented in Fig. 9.

Schlieren and direct-shadow photographs of the flow appear as Figs. 10 and 11 respectively.

These tests were made with transition-free boundary layers and no trace of shock-induced boundary-layer separation was observed in the photographs or could be deduced from the pressure distributions (incidences above $\alpha = 6$ deg were not obtainable since the tunnel became choked). It is concluded that at $M_0 = 1·40$ the boundary layers are of a naturally transitional type and are not strictly laminar at the beginning of the shock-wave boundary-layer interaction region.

3. *Conclusions*.—Shock-induced boundary-layer separation at the trailing edge of a 4 per cent thick biconvex aerofoil was present at $M_0 = 1·63$ with transition-free boundary layers but was absent at $M_0 = 1·63$ with transition-fixed boundary layers and at $M_0 = 1·40$ with transition-free boundary layers. The extent of the separated region confirmed the results given in Ref. 3.

Acknowledgements.—Mr. P. J. Peggs assisted in the experimental work and Mrs. N. A. North in the data reduction.

NOTATION

M_0	Tunnel free-stream Mach number
M	Local Mach number
θ	Flow deflection angle
α	Incidence of aerofoil
β	Trailing-edge semi-angle of aerofoil
c	Aerofoil chord
d	Length of separated flow region
δ_0^*	Calculated boundary-layer displacement thickness at beginning of separated region
C_N	Normal-force coefficient
C_m	Pitching-moment coefficient (about $0 \cdot 25$ chord)
p	Local static pressure
H_0	Stagnation pressure
x	Distance measured from leading edge of aerofoil.

REFERENCES

No.	*Author*	*Title, etc.*
1	B. D. Henshall and R. F. Cash	Observations of the flow past a two-dimensional 4 per cent thick biconvex aerofoil at high subsonic speeds. R. & M. 3092. February, 1957.
2	B. D. Henshall and R. F. Cash	An experimental investigation of leading-edge flow-separation from a 4 per cent thick two-dimensional biconvex aerofoil. R. & M. 3091. February, 1957.
3	B. D. Henshall and R. F. Cash	The interaction between shock waves and boundary layers at the trailing edge of a double wedge aerofoil at supersonic speed. R. & M. 3004. March, 1955.
4	G. E. Gadd, D. W. Holder and J. D. Regan	An experimental investigation of the interaction between shock waves and boundary layers. *Proc. Roy. Soc.* A. Vol. 226, pp. 227 to 253. 1954.
5	D. W. Holder, G. E. Gadd, H. H. Pearcey (N.P.L.) and J. Seddon (R.A.E.).	The interaction between shock waves and boundary layers (with a note on 'The effects of the interaction on the performance of supersonic intakes'). C.P. 180. February, 1954.

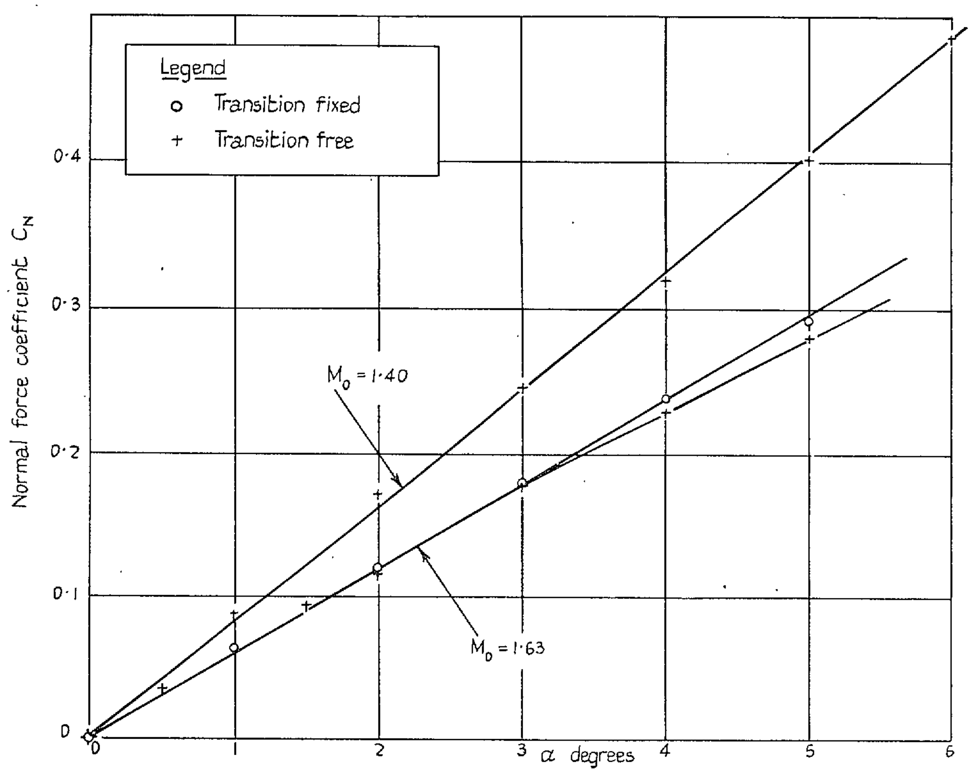

FIG. 1. Variation of normal-force coefficient C_N with incidence for 4 per cent biconvex aerofoil at $M_0 = 1\cdot63$ and $M_0 = 1\cdot40$.

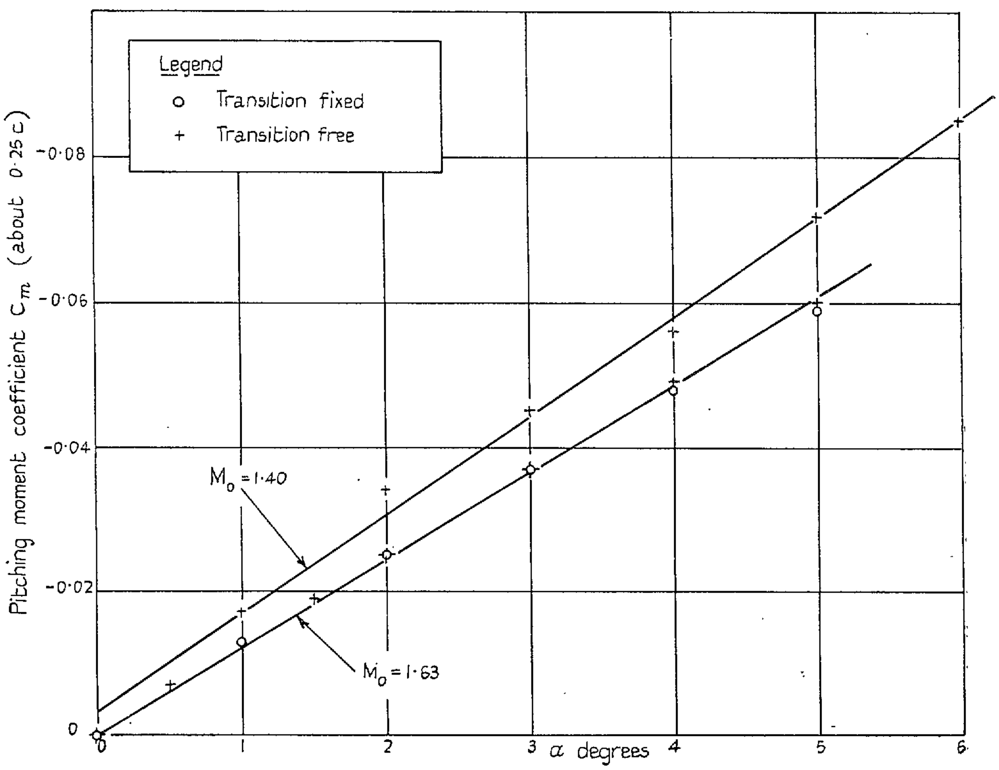

FIG. 2. Variation of pitching-moment coefficient C_m with incidence for 4 per cent biconvex aerofoil at $M_0 = 1\cdot63$ and $M_0 = 1\cdot40$.

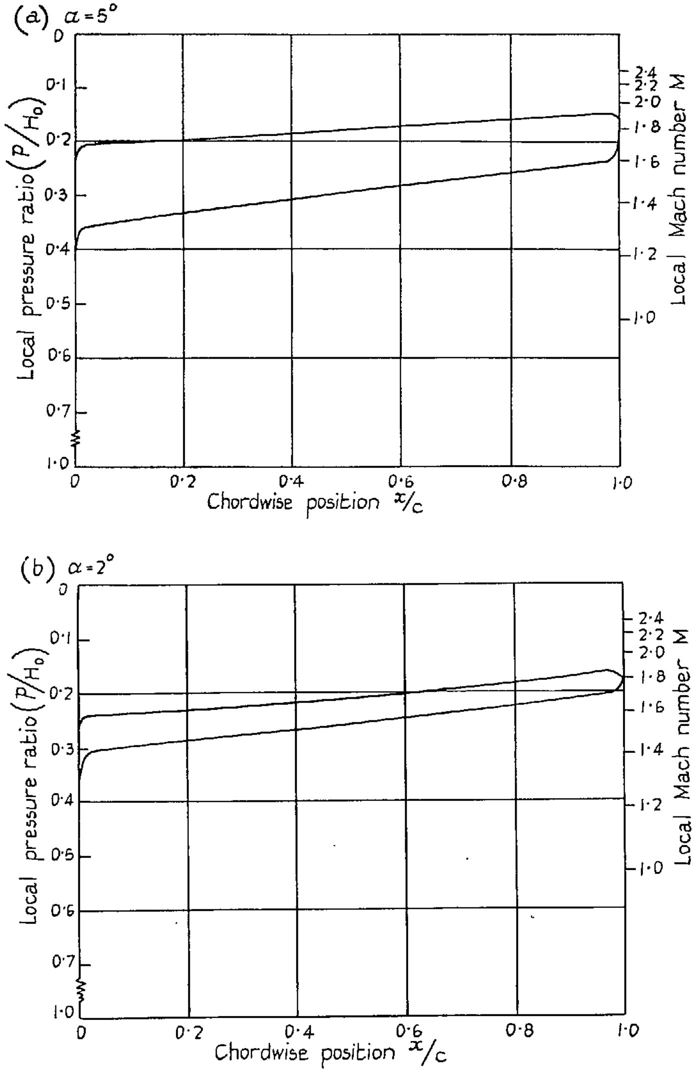

FIGS. 3a and 3b. Averaged pressure distributions for a 4 per cent biconvex aerofoil at $M_0 = 1 \cdot 63$ with 'transition-free' boundary layers.

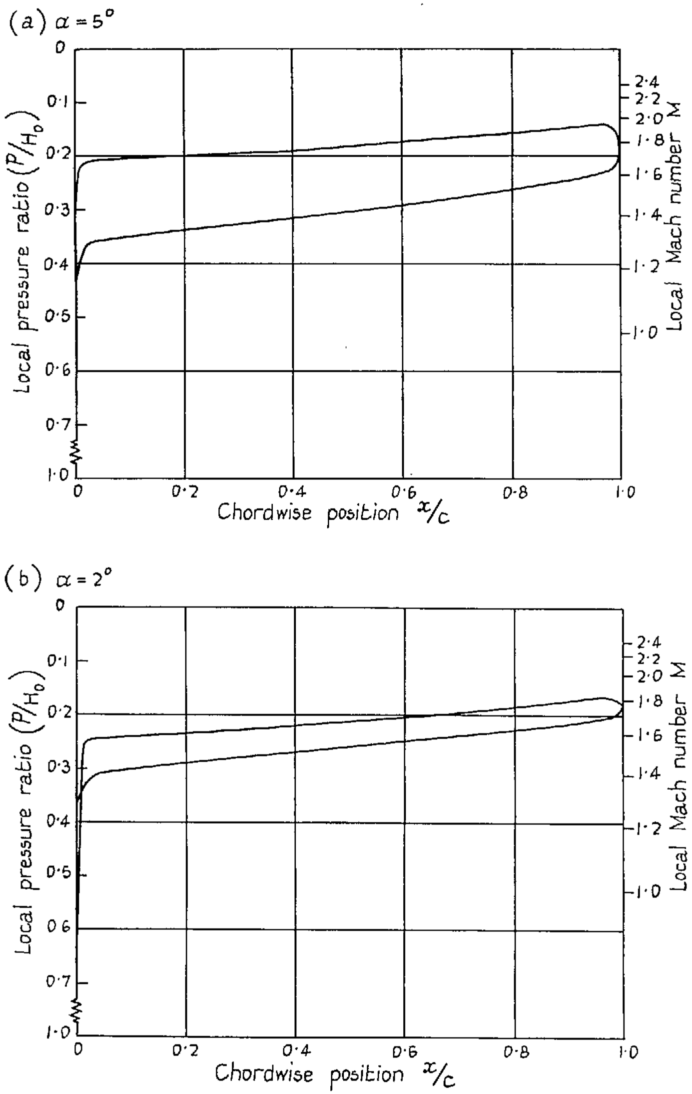

FIGS. 4a and 4b. Averaged pressure distributions for a 4 per cent biconvex aerofoil at $M_0 = 1 \cdot 63$ with 'transition-fixed' boundary layers.

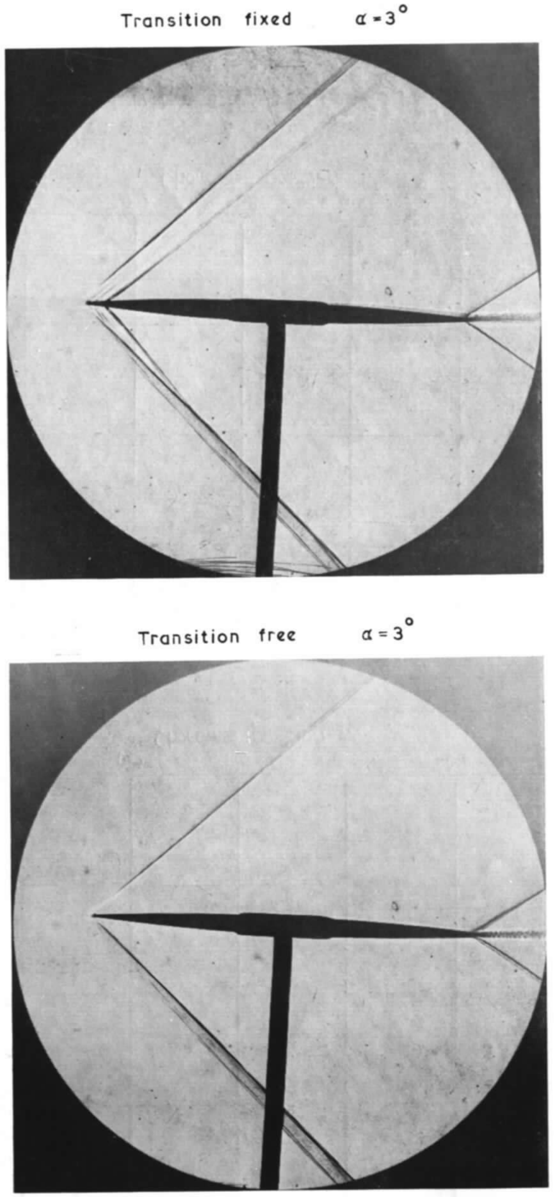

FIG. 5. Schlieren photographs of the flow past a 4 per cent thick biconvex aerofoil at $M_0 = 1\cdot63$.

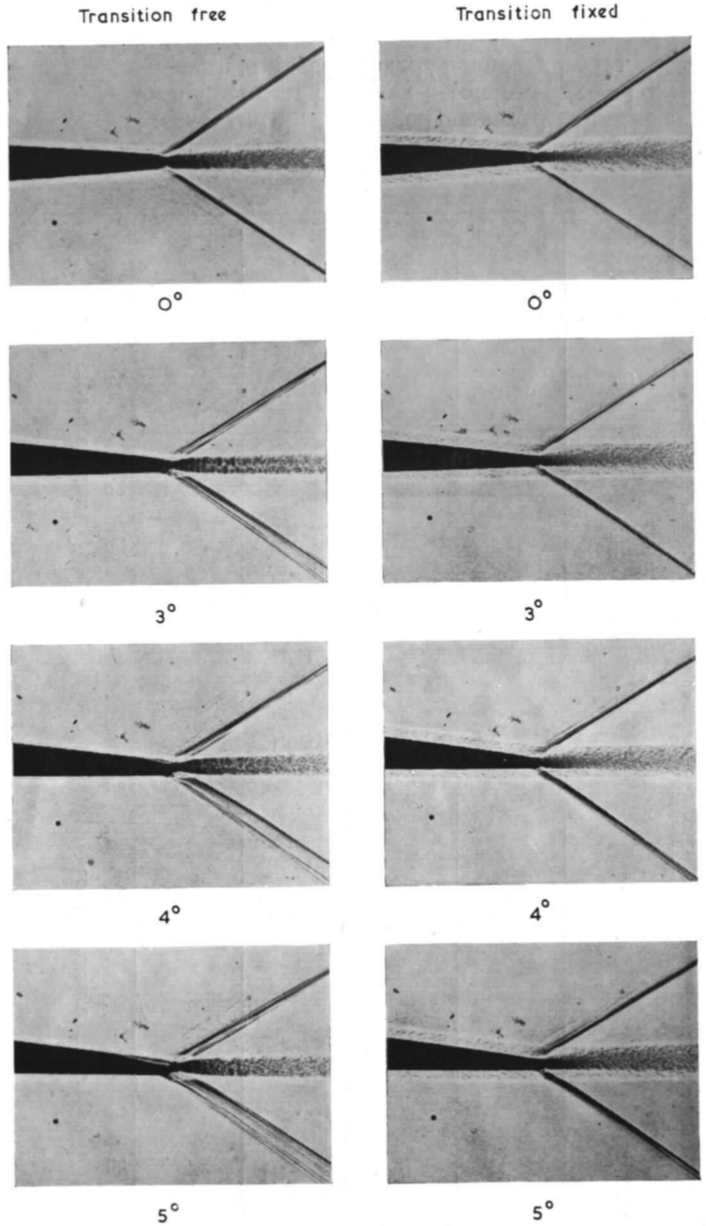

FIG. 6. Direct-shadow photographs of the flow past a 4 per cent thick biconvex aerofoil at $M_0 = 1\cdot63$.

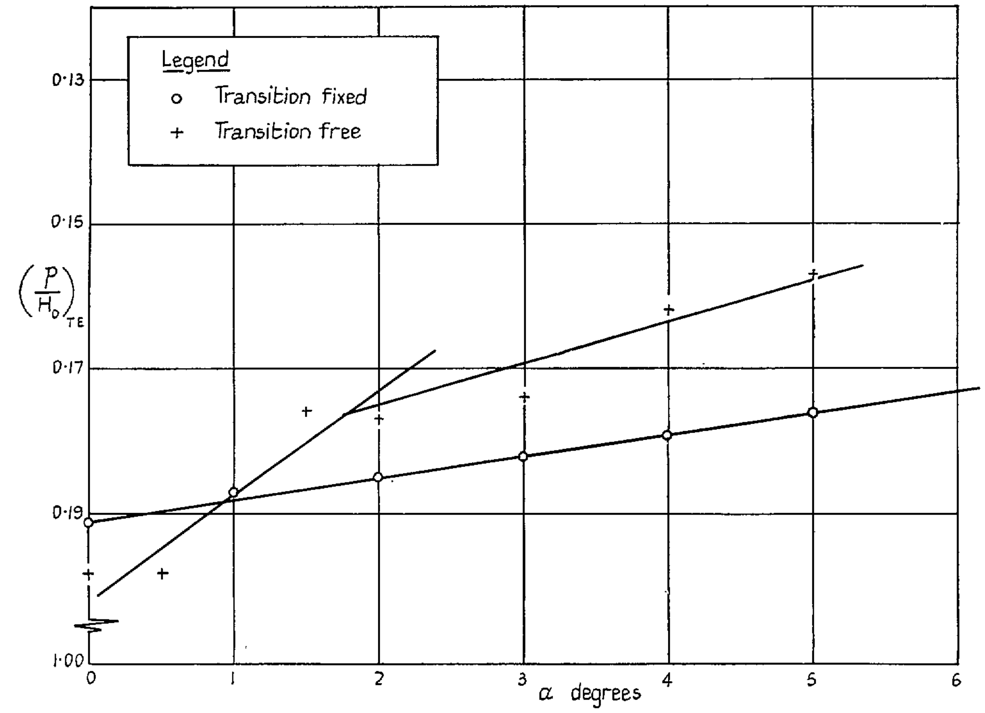

FIG. 7. Variation of the pressure ratio (p/H_0) at the trailing edge with incidence for 4 per cent biconvex aerofoil at $M_0 \doteq 1 \cdot 63$.

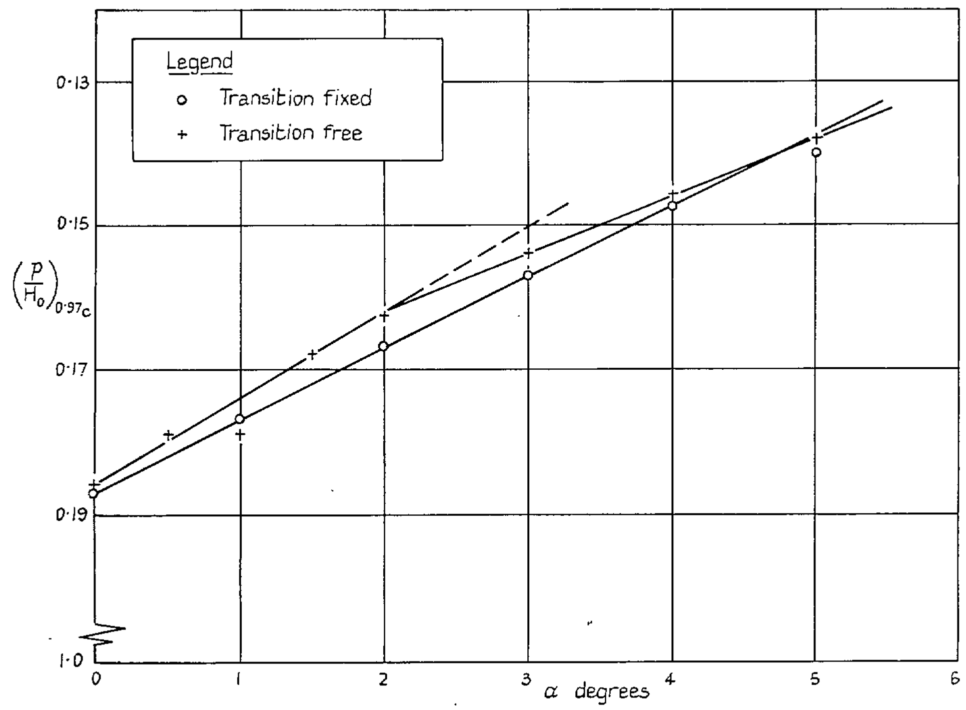

FIG. 8. Variation of the pressure ratio (p/H_0) at $0 \cdot 97c$ with incidence for 4 per cent biconvex aerofoil at $M_0 = 1 \cdot 63$.

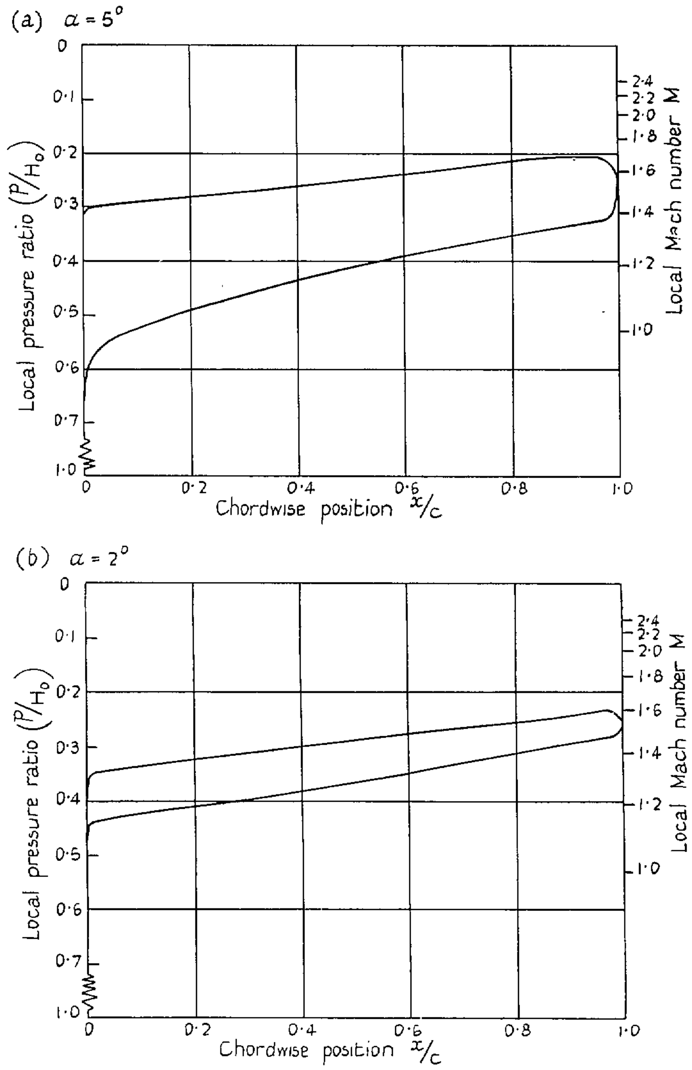

FIGS. 9a and 9b. Averaged pressure distributions for a 4 per cent biconvex aerofoil at $M_0 = 1 \cdot 40$ with 'transition-free' boundary layers.

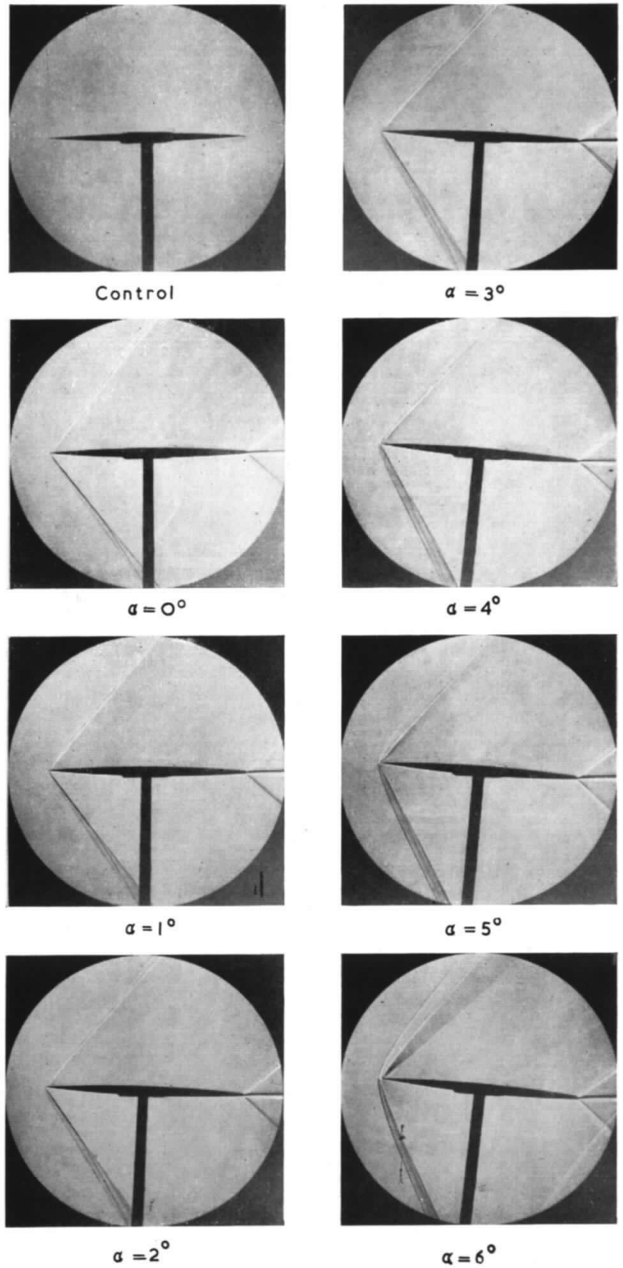

FIG. 10. Schlieren photographs of the flow past a 4 per cent thick biconvex aerofoil at $M_0 = 1 \cdot 40$.

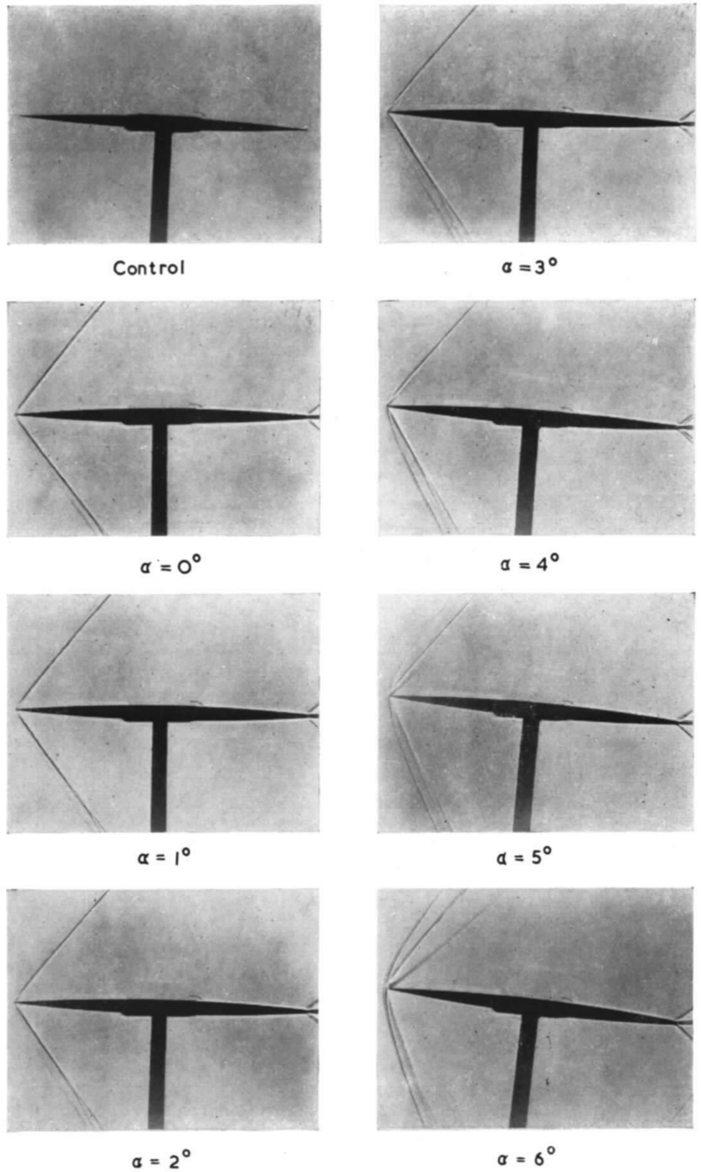

FIG. 11. Direct-shadow photographs of the flow past a 4 per cent thick biconvex aerofoil at $M_0 = 1 \cdot 40$.

(73270) Wt. 53/2293 K7. 8/58 Hw.

PRINTED IN GREAT BRITAIN

Publications of the Aeronautical Research Council

ANNUAL TECHNICAL REPORTS OF THE AERONAUTICAL RESEARCH COUNCIL (BOUND VOLUMES)

1939 Vol. I. Aerodynamics General, Performance, Airscrews, Engines. 50s. (52s.).
Vol. II. Stability and Control, Flutter and Vibration, Instruments, Structures, Seaplanes, etc. 63s. (65s.)

1940 Aero and Hydrodynamics, Aerofoils, Airscrews, Engines, Flutter, Icing, Stability and Control, Structures, and a miscellaneous section. 50s. (52s.)

1941 Aero and Hydrodynamics, Aerofoils, Airscrews, Engines, Flutter, Stability and Control, Structures. 63s. (65s.)

1942 Vol. I. Aero and Hydrodynamics, Aerofoils, Airscrews, Engines. 75s. (77s.)
Vol. II. Noise, Parachutes, Stability and Control, Structures, Vibration, Wind Tunnels. 47s. 6d. (49s. 6d.)

1943 Vol. I. Aerodynamics, Aerofoils, Airscrews. 80s. (82s.)
Vol. II. Engines, Flutter, Materials, Parachutes, Performance, Stability and Control, Structures. 90s. (92s. 9d.)

1944 Vol. I. Aero and Hydrodynamics, Aerofoils, Aircraft, Airscrews, Controls. 84s. (86s. 6d.)
Vol. II. Flutter and Vibration, Materials, Miscellaneous, Navigation, Parachutes, Performance, Plates and Panels, Stability, Structures, Test Equipment, Wind Tunnels. 84s. (86s. 6d.)

1945 Vol. I. Aero and Hydrodynamics, Aerofoils. 130s. (132s. 9d.)
Vol. II. Aircraft, Airscrews, Controls. 130s. (132s. 9d.)
Vol. III. Flutter and Vibration, Instruments, Miscellaneous, Parachutes, Plates and Panels, Propulsion. 130s. (132s. 6d.)
Vol. IV. Stability, Structures, Wind Tunnels, Wind Tunnel Technique. 130s. (132s. 6d.)

Annual Reports of the Aeronautical Research Council—

1937 2s. (2s. 2d.) 1938 1s. 6d. (1s. 8d.) 1939–48 3s. (3s. 5d.)

Index to all Reports and Memoranda published in the Annual Technical Reports, and separately—

April, 1950 - - - - R. & M. 2600 2s. 6d. (2s. 10d.)

Author Index to all Reports and Memoranda of the Aeronautical Research Council—

1909—January, 1954 R. & M. No. 2570 15s. (15s. 8d.)

Indexes to the Technical Reports of the Aeronautical Research Council—

December 1, 1936—June 30, 1939	R. & M. No. 1850	1s. 3d. (1s. 5d.)
July 1, 1939—June 30, 1945	R. & M. No. 1950	1s. (1s. 2d.)
July 1, 1945—June 30, 1946	R. & M. No. 2050	1s. (1s. 2d.)
July 1, 1946—December 31, 1946	R. & M. No. 2150	1s. 3d. (1s. 5d.)
January 1, 1947—June 30, 1947	R. & M. No. 2250	1s. 3d. (1s. 5d.)

Published Reports and Memoranda of the Aeronautical Research Council—

Between Nos. 2251–2349	R. & M. No. 2350	1s. 9d. (1s. 11d.)
Between Nos. 2351–2449	R. & M. No. 2450	2s. (2s. 2d.)
Between Nos. 2451–2549	R. & M. No. 2550	2s. 6d. (2s. 10d.)
Between Nos. 2551–2649	R. & M. No. 2650	2s. 6d. (2s. 10d.)
Between Nos. 2651–2749	R. & M. No. 2750	2s. 6d. (2s. 10d.)

Prices in brackets include postage

HER MAJESTY'S STATIONERY OFFICE

York House, Kingsway, London W.C.2; 423 Oxford Street, London W.1; 13a Castle Street, Edinburgh 2; 39 King Street, Manchester 2; 2 Edmund Street, Birmingham 3; 109 St. Mary Street, Cardiff; Tower Lane, Bristol 1; 80 Chichester Street, Belfast, *or through any bookseller.*

S.O. Code No. 23-3093